

Synthesis of Reduced Graphene Oxide-Titanium (rGO-TiO₂) Composite Using a Solvothermal and Hydrothermal Methods and Characterized via XRD and UV-Vis

Huzaikha Awang, Nurul Infaza Talalah

PPSTUMS Sabah Malaysia, UITM Pahang Malaysia, Jengka, Pahang, Malaysia

Email: huzaikha.ikha@ums.edu.my, nurulinfaza@uitm.edu.my

How to cite this paper: Awang, H. and Talalah, N.I. (2019) Synthesis of Reduced Graphene Oxide-Titanium (rGO-TiO₂) Composite Using a Solvothermal and Hydrothermal Methods and Characterized via XRD and UV-Vis *Natural Resources*, 10, 17-28.

<https://doi.org/10.4236/nr.2019.102002>

Received: January 3, 2019

Accepted: February 23, 2019

Published: February 26, 2019

Copyright © 2019 by author(s) and Scientific Research Publishing Inc.

This work is licensed under the Creative Commons Attribution International License (CC BY 4.0).

<http://creativecommons.org/licenses/by/4.0/>



Open Access

Abstract

Nowadays, Carbon Capture and Conversion (CCC) method is one of the alternative solutions in carbon management. The reduced graphene oxide-Titanium (rGO-TiO₂) composites are the CCC material that will capture the carbon dioxide (CO₂) and convert it into hydrocarbon fuels such as methane. The effect of synthesizing method into crystallinity growth and the band gap will be studied in this research work. Therefore, the rGO-TiO₂ will be synthesized via solvothermal and hydrothermal methods and then will be characterized via XRD and UV-Vis. The temperature and treatment time were fixed in both synthesis methods. The characterization results via XRD and UV-Vis conclude that, the different synthesis methods affected the crystallinity growth and its band gap. The rGO-TiO₂ synthesized via modified hydrothermal method shows the lowest crystallite size and band gap compared to other samples. It will indirectly affect the photogenerated electrons on TiO₂ to rGO better compared to rGO-TiO₂ synthesized via solvothermal. The green synthesis method which requires a low equipment cost and simple experimental steps is the contribution of this research finding.

Keywords

Component, Formatting, Style, Styling

1. Introduction

Current energy infrastructures which mostly depend on fossil fuels release greenhouse gases (GHG) and lead to the global warming. According to Wallington *et al.*, 30 billions of tons CO₂ emissions were released every year general-

ly for the electricity and heat production [1]. Besides that, the global energy demand is forecasted to increase in the future with the growth by roughly double in 2050 and triple by the end of this century [2]. Therefore, meeting the current energy demand and reducing the impact of global warming are two global issues that really need an appropriate solution. Nowadays, the alternative solutions in carbon management are Carbon Capture and Storage (CCS) and Carbon capture and Utilization (CCU). The CCS is known as the long term solutions but it has a high potential hazard due to CO₂ leakage and high equipment cost [3]. The CCU method reuses the captured CO₂ but it is only applicable for a high purity of CO₂ waste. Therefore, the new alternative was introduced, the Carbon Capture and Conversion (CCC) method. This CCC method will convert the captured CO₂ into a renewable energy product such as methane, ethane, ethylene and methanol. This new alternative is promptly able to meet the global energy demand without any fossil fuels shortages and has a high potential energy source since CO₂ is green, abundant, nontoxic and an inexpensive feedstock [4] [5]. Since this method is new and not commercial yet, some improvements need to be done. The highly efficient CCC materials synthesized via a green method with a low equipment cost and simple experimental steps are the ultimate goals in this research work.

The morphological change such as surface area and the crystallinity phase will affect the photocatalytic efficiency in each composite and this morphological change is actually related to the synthesis method [6]. According to Rosa M. *et al.*, highly efficient CCC materials with a longer lifespan can be synthesized by focusing on the synthesis method [7]. According to Dong *et al.*, although the chemical modification of TiO₂-carbon composite can enhance the capability to absorb in the visible range and improve its photocatalytic performance, it can also decrease the surface area and thereby decrease the absorptive power and photocatalytic performance. That is because of the weak interfacial contact GO and severe aggregation of TiO₂ particles on the graphene sheets, causing the development of highly efficient photocatalyst remains challenging until today.

There were various synthesis methods that had been reported such as simple liquid phase deposition method [8], thermal hydrolysis of suspension [9], simple wet impregnation method [10], microwave-hydrothermal treatment [11], simple solvothermal method [12] and modified hydrothermal method [13] [14] which were using different raw material, equipment needed and also different experimental step. Based on our study, we found that the solvothermal and hydrothermal method are the good synthesis method due to their availability and low raw material cost, low equipment cost and also the simple and scalable experimental step. The differences between the solvothermal and hydrothermal synthesis methods are only the solvent used. The solvothermal typically using an acid such as acetic acid while hydrothermal using alkaline water or distilled water as a solvent. Solvent is important aspect in both morphological growths since it will control the state of active Ti species during the growth. According to Shen, *et al.*, the obtained rGO-TiO₂ composite via a modified hydrothermal me-

thod are pure, with less defects compared to others synthesized method, controllable structure and quite high CO₂ conversion rate [6]. Wang *et al.* reported that, the in-situ hydrothermal method can ensure the strong interaction between the semiconductor nanocomposites which makes their work synergistically [15]. Besides that, Zhang *et al.* reported that, the hydrothermal method to synthesize the TiO₂-GO is the simple and efficient method [16]. According to the Fan and co, the TiO₂-rGO composites which prepared by the hydrothermal method shows the most efficient photocatalyst for the evolution of H₂ compare to others synthesize method; UV-assisted photoreduction and chemical reduction using a hydrazine [17]. In contrast, [12] reported that the solvothermal method is economically and practically feasible method. Ali *et al.*, reported that the solvothermal method are the most effective, cleaner route, economic and environmentally friendly [18].

The effects of synthesis method on the growth of reduced graphene oxide-Titanium (rGO-TiO₂) as a Carbon Capture and Conversion (CCC) composite will be studied. The rGO-TiO₂ composites in this research works were synthesized via solvothermal and hydrothermal methods. The CCC composite will then be analyzed by using a UV-Vis and XRD. By focusing on the synthesizing method of this CCC composite, it will give a great contribution and beneficiaries to the renewable energy fields.

2. Material and Method

2.1. Materials

The raw material been used to prepare the rGO-TiO₂ composites are Graphite Oxide (GO) powder, Tetrabutyl Titanate powder (TBT), commercial TiO₂ Anatase powder, ethylene glycol (EG), acetic acid (HAc) and Ammonium hydroxide (NaOH).

2.2. Characterization

There are several characterizations equipment had been used such as Field Emission Scanning Electron Microscopy (FESEM) to check the surface morphology, X-ray Diffractometry (XRD) to check the crystallinity, UV-Vis spectrophotometer to identify the optical properties, Electrochemical Impedance Spectroscopy (EIS) to check the electrical properties, Fluorescent spectrometer (PL) to check the recombination rate of the photogenerated electron-hole pairs and lastly is the Gas Chromatograph (GC) to testing the photo reduction and conversion. In this paper, the results obtained from the XRD and UV-Vis were focused on.

The crystallinity of the samples, rGO-TiO₂ composites will be examine by using XRD with the radiation (wavelength, $\lambda = 0.15406$ nm) at $0.02^\circ \text{ s}^{-1}$ a scan rate (2θ). The absorbance spectra were analyzed by using a UV-Vis spectroscope under ambient temperature in the wavelength ranging from 200 - 800 nm. The band gap energies of the photocatalyst were estimated from the Kubelka-Munk

(KM) function $F(R)$ and the extrapolation of the Tauc plot $[F(R) \cdot hv]^{1/2}$ to the abscissa of photon energy, hv . The raw data were analyzed by using the Origin-Pro 9.1 and excel software to tabulate and plotting the graphs. Four samples will be compared; pure TiO_2 , $rGO-TiO_2$ (S), $rGO-TiO_2$ (H1) and $rGO-Anatase TiO_2$ (H2). The $rGO-TiO_2$ (S) was synthesized by solvothermal while $rGO-TiO_2$ (H1) and $rGO-Anatase TiO_2$ (H2) were synthesized by hydrothermal method.

2.3. Synthesis Method

The solvothermal method (S) were using a step reported by [10], the hydrothermal method 1 (H1) were using a modification of method reported by [10]. The modification of step [10] is followed by [19]. The hydrothermal method 2 (H2) are followed the method reported by [20]. The (H1) method is originally proposed in this research work to synthesize the $rGO-TiO_2$ composite for photocatalyst reduction applications. To the best of our knowledge, there is no reported paper which synthesized the $rGO-TiO_2$ composite by using this H1 method. The solvent used in the (S) method are the ethylene glycol (EG) and acetic acid (HAc) as per [10] while the (H1) method are NaOH and distilled water as the alkaline solvent before heated in autoclave at $180^\circ C$ temperature. The 8 hours treatment time in autoclave and $180^\circ C$ temperature were fixed conditions for both solvothermal and hydrothermal methods. The effect of synthesis method on the crystallinity, recombination rate of electron-hole pairs and photocatalytic activities in each synthesized composites will be study and discuss further.

2.4. Synthesis of Graphene Oxide (GO)

Figure 1 shows the synthesizing process of graphene oxide (GO) from the graphite powder by using a modified Hummers method [12]. Graphite powder were added into concentrated H_2SO_4 , P_2O_5 and $K_2S_2O_8$ then undergo the mixture, filter and wash process and dried overnight. On the next day, the pre-oxidized graphite was dispersed into cold ($0^\circ C$) concentrated H_2SO_4 . $KMnO_4$ were added slowly until thick green paste was observed. The residue then was filtered, washed, and kept overnight. The solution was then centrifuged at 14000rpm for 30 min each time to obtain the GO powder.



Figure 1. Synthesis of Graphene Oxide (GO).

2.5. Synthesis of rGO-TiO₂ Composite via Solvothermal Method, rGO-TiO₂ (S)

Figure 2 shows the synthesizing process of rGO-TiO₂ (S) via a solvothermal method by using a Teflon-Lined autoclave. The TiO₂ precursor was synthesized from the TBT powder. The GO sheet was prepared by dispersing the GO into distilled water and ultrasonicated for 1 hour at ambient temperature. The GO sheet solution was chilled until to $\approx 5^{\circ}\text{C}$ in an ice bath and labelled as solution A. The titanium solution was prepared by adding the TiO₂ precursor, ethylene glycol (Eg) and acetic acid (HAc) together. The TiO₂ solution was then chilled to $\approx 5^{\circ}\text{C}$ in an ice bath and labelled as solution B. Consequently, the solution B was added dropwise into the chilled solution A under vigorous stirring. The mixture of solution A and B was then transferred into 200 mL Teflon Lined stainless steel autoclave and was heated for 8 hours. The resultant solid was dried in air oven overnight. Before the characterization stage, the precipitate was annealed for 60 minutes.

2.6. Synthesis of rGO-TiO₂ Composite via Hydrothermal Method, rGO-TiO₂ (H1) and rGO-Anatase TiO₂ (H2)

Figure 3 shows the synthesizing process of rGO-TiO₂ (H1) and rGO-TiO₂ (H2) via a Hydrothermal Method by using a Teflon-Lined autoclave. The rGO-TiO₂ (H1) was synthesized from the TBT powder while rGO-TiO₂ (H2) from the P90 TiO₂ powder. The GO sheet was prepared by sonicating the GO mixture which consist of GO and deionized water for 1 hour. Then, add TiO₂ precursor powder dropwise into the stirring GO mixture. The mixture was further stirred for 1 hour to ensure complete mixing. Next, the NaOH was then added into the mixture. The solution was then transferred into 200 mL Teflon-Lined autoclave and heated under static condition for 8 hours. The gray colored gel product was then washed with 0.1M HCl solution and stirred overnight at room temperature. Subsequently, the final product was washed with deionized water several times, centrifuged at 5000 rpm for 30 minutes and dried overnight. Before the characterization stage, the precipitate was annealed 300°C for 60 minutes.



Figure 2. Synthesis rGO-TiO₂ (S) via solvothermal method by using a Teflon-Lined autoclave.



Figure 3. Synthesis rGO-TiO₂ (H1) and rGO-TiO₂ (H2) via hydrothermal method by using a Teflon-Lined autoclave.

3. Results and Discussion

The crystallinity of chemical composition and the crystalline size of composites can be determined by using XRD. Higher the crystallinity and smaller the crystalline size will lead to the better photocatalytic performance.

The interaction between rGO and TiO₂ can be analyze in the diffuse reflectance of UV-Vis result. The wavelength (nm) in the absorption edge was indicate the elemental band gap absorption of TiO₂ from the electron transitions from VB to the CB [18]. The higher the wavelength (nm) in the absorption edge means lower the elemental band gap absorption of its TiO₂ which lead to the better photocatalytic performance because the electron at the VB do not need to absorb high energy from the UV light to excite and escape to the CB. Besides that, by using the Tauc plot of the modified Kubelka-Munk (KM) function with a linear extrapolation, we can determine the optical bandgap of each composite.

3.1. XRD

Figure 4 shows the XRD patterns of (S), (H1) and (H2). The note A means the TiO₂ in anatase phase while R means in rutile phase. The XRD pattern of (S) above shows the significant peaks at 25.3°, 27.439°, 37.8° and 48° which can be indexed to the (101A), (101R), (004) and (200) crystal planes of a tetragonal anatase phase (JCPDS no. 21-1272) [12]. The XRD patterns of the (H2) above shows the significant peaks at 25.3° and 48° which are match with the titanium anatase pattern (ICSD ref no. 00-004-0477) with the lattice constants $a = 3.7830 \text{ \AA}$ and $c = 9.5100 \text{ \AA}$. Besides that, there is another peak at 27.439° which was matched with the titanium rutile pattern (ICSD ref no. 01-078-1508) with the lattice constants $a = 4.5933 \text{ \AA}$ and $c = 2.9580 \text{ \AA}$. It means that the composite are consist of both anatase and rutile phase TiO₂. However, the crystallinity peak of this composite shows the lowest peak compare to the other composites (S) and (H1) which lead to the lowest crystallinity and biggest crystalline size.

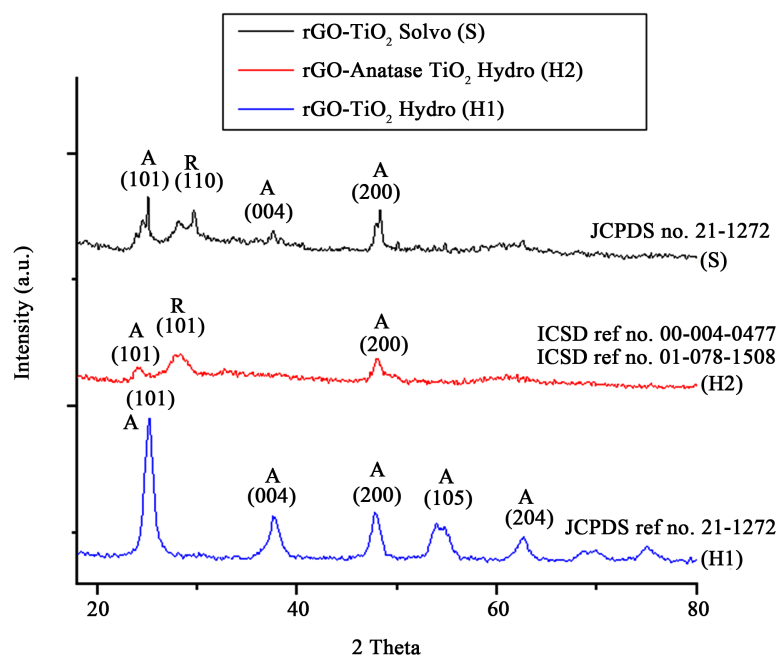


Figure 4. XRD patterns of rGO-TiO₂ (S), rGO-TiO₂ (H1) and rGO-Anatase TiO₂ (H2).

The XRD patterns of the (H1) above shows several peaks at 25.3° (101), 37.8° (004), 48° (200), 53.9° (105), 62.7° (204), 70.3° (116) and 75° (215) which match with the pure tetragonal anatase phase (JCPDS ref no. 21-1272) with the lattice constants $a = 3.78 \text{ \AA}$ and $c = 9.50 \text{ \AA}$. The diffraction peak of rGO-TiO₂ (H1) showed a strong and sharp diffraction peak which lead to the highest crystallinity and the smallest crystalline size. Referring to the XRD result reported by Wenqing *et al.*, the rGO diffraction peak are at 24.5° with the very broad peak and looks disappear [13]. The rGO were stacked together with the TiO₂ nanoparticles to form the undetectable graphite structure [13]. Therefore, we assume that our undetectable rGO diffraction peak was being shielded by the main peak of anatase TiO₂ at 25.3°. We can conclude that, all composites were pure and well crystallized due to no diffraction peak was detected from the impurities compositions. The rGO-TiO₂ composites prepared by the other methods showed similar XRD patterns [12] [13].

The broad diffraction peaks are indicating the big crystallite size while the sharp and strong diffraction peaks determine the small crystallite size. As mention earlier, the smaller the crystalline size, the better its photocatalytic performance. That is because, the small crystallite size will provide a big surface area which is the most important for the photocatalytic activity to occur. By using the Scherrer's equation as shown in Equation (1) below, we calculate the average crystal size of the TiO₂ particles in each composite for further analyzation. The λ is the CuK α radiation ($\lambda = 0.15406 \text{ nm}$), β is the full width at half maximum (FWHM) intensity of the peak in radians and θ is the Bragg's diffraction angle.

$$D = \frac{0.9\lambda}{\beta \cos \theta}$$

Equation (1): Scherrer’s equation [15].

Figure 5 shows the average crystal size of the TiO₂ particles in (S), (H1) and (H2) composite by using a Scherrer’s equation. The average crystal size of the TiO₂ particles in the (S), (H1) and (H2) composites are 86.57 nm, 107.05 nm and 42.14 nm respectively. Clearly shows that the crystallinity and the crystal size of TiO₂ were affected by the synthesizing method. The crystallinity and the better crystallite size was at (H1) composite. The smallest crystallite size means the biggest surface area for a better photocatalytic performance.

3.2. UV-Vis

Figure 6 shows the UV Vis diffuse reflectance spectra of titanium (TiO₂), (H2), (S) and (H1). As shown in Figure 4, the estimated wavelength in absorption edge for the spectra (TiO₂), (H2), (S) and (H1) are 390 nm, 410 nm, 420 nm and 490 nm respectively. Notably that the synthesized rGO-TiO₂ composites (H2), (S) and (H1) were shifted to the higher wavelength in the absorption edge compare to the pure titanium (TiO₂).

Figure 7 shows the Kubelka-Munk function plot of (TiO₂), (H2), (S) and (H1). We can see the approximated band gaps of (TiO₂), (H2), (S) and (H1)

CCC Composite	2θ	θ	Cos θ	Sin θ	FWHM(°)	FWHM (Radian)	B Cos θ	Particle Size (nm)
rGO-TiO ₂ (S)	25.2806	12.6403	0.9973	0.0739	0.092	0.0016	0.0016	86.57
rGO-TiO ₂ (H1)	25.2806	12.6403	0.9972	0.0739	0.0744	0.0013	0.0013	107.05
rGO-Anatase TiO ₂ (H2)	25.2806	12.6403	0.9973	0.00739	0.189	0.0033	0.0033	42.14

Figure 5. The crystal size of the TiO₂ particles in rGO-TiO₂ (S), rGO-TiO₂ (H1) and rGO-Anatase TiO₂ (H2) composites.

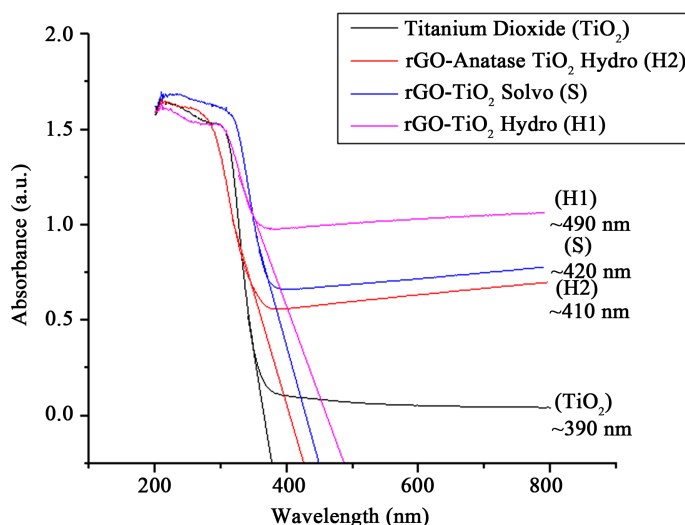


Figure 6. UV Vis diffuse reflectance spectra of titanium (TiO₂), rGO-Anatase TiO₂ (H2), rGO-TiO₂ (S) and rGO-TiO₂ (H1).

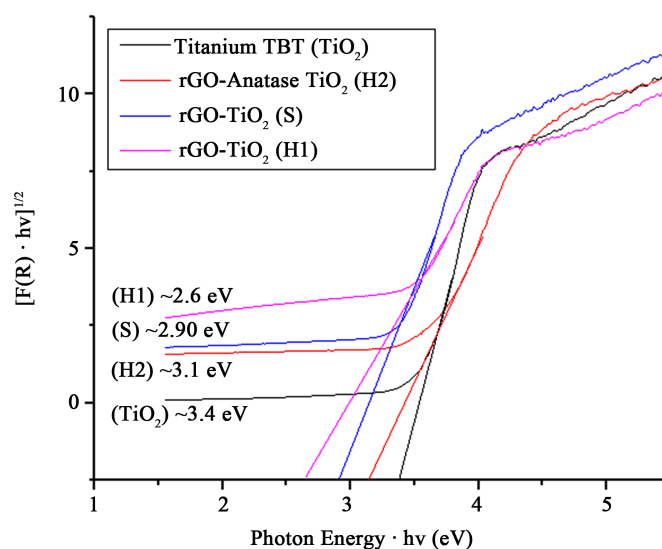


Figure 7. Kubelka-Munk function plot of titanium (TiO₂), rGO-Anatase TiO₂ (H2), rGO-TiO₂ (S) and rGO-TiO₂ (H1).

are 3.40 eV, 3.10 eV, 2.90 eV, 2.60 eV respectively. Due to some researchers, the band gap narrowing occurs because of the formation of strong Ti-O-C bond between the TiO₂ and rGO composites [21] [22]. The smaller the band gap, the better the formation of Ti-O-C bond due to the strong contact between TiO₂ and rGO. Based on this result, the formation of Ti-O-C bond in (H1) is the strongest compare to (S) and (H2) can be concluded. The formation of Ti-O-C bond leads to improve the absorption edge and resulting a better electron transitions from the VB to the CB for a better photocatalytic performance.

3.3. Discussion

As we can see from the UV Vis spectroscopy result, the band gap narrowing was showed for all three composites compare to pure TiO₂. The (H1) shows the lowest band gap with 2.60 eV compare to the (S) with 2.90 eV and (H2) with 3.10 eV. Hence, the possibility of (H1) composite to perform a better photocatalytic reduction is high compare (H2) and (S) due to its wider absorption light range and potentially to produce a multiple photogenerated electron-hole pairs. The strong interaction/contact between TiO₂ and rGO will form a better Ti-O-C bond and lead to the band gap narrowing [21] [22]. Perera *et al.* stated that, the presence of rGO can help to separate the photogenerated electron-hole pairs and without them, the possibility of the photogenerated electron-hole pairs to recombine is high [14].

In addition, according to the Liang *et al.*, and Fan W. *et al.*, the formation of Ti-O-C chemical bonding in the graphene-TiO₂ composites lead to control the morphology of TiO₂ nanoparticles on the graphene sheets [21] [22]. The best formation of Ti-O-C chemical bonding in (H1) caused it has the best morphology (less agglomerate and high crystallinity). The (H1) composite also shows the best crystallinity and smallest crystallite size with ~42 nm compare to the other

composites, (H2) with ~107 nm and (S) with ~86 nm. The smallest crystal size of (H1) composite means it provide the biggest surface area which leads to the better photoreduction performance.

Even though this research study is only study two synthesis conditions, but it still means a lot to the wider photocatalyst field especially for this new rGO-TiO₂ composite as a photocatalyst reduction of CO₂ into CH₄ applications. The synthesis method that we used to synthesis the (H1) is originally propose by us and not yet reported by previous researchers. This method only uses the GO powder, TBT powder and NaOH as a raw material. The NaOH and distilled water as the solvent prove that this method are green and environmentally friendly since it do not produce any acidic waste which can harm our environment after the synthesis process compare to the solvothermal method which need some acetic acid (HAc) as the solvent. This method also use a low equipment cost since it only need an autoclave for its simple experimental steps. This project could make a great contribution in investigating the best synthesizing method to synthesis a high efficient CCC composite via a green raw material, low equipment cost and simple experimental step.

4. Conclusion

The growth and properties of rGO-TiO₂ composites which were synthesized by three different conditions: (S), (H1) and (H2) have been successfully studied. The effect of synthesizing method via solvothermal and hydrothermal methods was examined and analyzed by UV Vis and XRD. The results show that the samples had different growth, purity, crystallite size and band gap, leading to different photocatalyst performances. From the results obtained, the (H1) composite has a strongest interaction between TiO₂ and rGO sheets in the composite due to its significant strong Ti-O-C peak and lowest band gap (2.60 eV) compared to the (H2) and (S). The intimate contact between the TiO₂ and rGO may accelerate the transfer of photogenerated electrons on TiO₂ to rGO and decelerate the recombination of charge carriers. The synthesis method and a pure TBT TiO₂ are the main reasons of its better performance compared to other samples. Several characterizations are suggested in further work in order to strengthen these findings. The future characterizations are such as Field Emission Scanning Electron Microscopy (FESEM) to check the surface morphology, Electrochemical Impedance Spectroscopy (EIS) to check the electrical properties, Fluorescent spectrometer (PL) to check the recombination rate of the photogenerated electron-hole pairs and lastly the Gas Chromatograph (GC) to test the photo reduction and conversion. We believe that, this approach could help to produce a high grade of rGO-TiO₂ at a large scale in the future due to its green and environmentally friendly raw material, low equipment cost and also simple and efficient experimental works.

Acknowledgements

Thanks to Heriot Watt University Malaysia (HWUM) for this collaboration with

Monash University Malaysia. The laboratory work was conducted at chemical engineering research lab, Monash University Malaysia. The software to analyze raw data such as Origin 9.1 and excel had been provided by HWUM and PPST, University Malaysia Sabah (UMS).

Conflicts of Interest

The authors declare no conflicts of interest regarding the publication of this paper.

References

- [1] Young, G.O. (1964) Synthetic Structure of Industrial Plastics. Peters, J., Ed. 2nd Edition, McGraw-Hill, New York, 15-64.
- [2] Chen, W.-K. (1993) Linear Networks and Systems. Wadsworth, Belmont, CA, 123-135.
- [3] Poor, H. (1985) An Introduction to Signal Detection and Estimation. Springer-Verlag, New York, Ch. 4.
- [4] Yorozu, Y., Hirano, M., Oka, K. and Tagawa, Y. (1982) Electron Spectroscopy Studies on Magneto-Optical Media and Plastic Substrate Interfaces. *IEEE Translation Journal on Magnetics in Japan*, **2**, 740-741.
<https://doi.org/10.1109/TJM.1987.4549593>
- [5] Duncombe, J.U. (1959) Infrared Navigation—Part I: An Assessment of Feasibility. *IEEE Transactions on Electron Devices*, **ED11**, 34-39.
- [6] Bingulac, S.P. (1994) On the Compatibility of Adaptive Controllers. *4th Annual Allerton Conference on Circuit and System Theory*, New York, 8-16.
- [7] Rosa, A.A., Cue'llar-Franca, M. (2015) Carbon Capture, Storage and Utilisation Technologies: A Critical Analysis and Comparison of Their Life Cycle Environmental Impacts. *Journal of CO₂ Utilization*, **9**, 82-102.
<https://doi.org/10.1016/j.jcou.2014.12.001>
- [8] Zhang, H., Xu, P., Du, G., Chen, Z., Oh, K., Pan, D. and Jiao, Z. (2011) A Facile One-Step Synthesis of TiO₂/Graphene Composites for Photodegradation of Methyl Orange. *Nano Research*, **4**, 274-283. <https://doi.org/10.1007/s12274-010-0079-4>
- [9] Stengl, V., Bakardjieva, S., Grygar, T.M., Bludská, J. and Kormunda, M. (2013) TiO₂-graphene Oxide Nanocomposite as Advanced Photocatalytic Materials. *Chemistry Central Journal*, **7**, 41. <https://doi.org/10.1186/1752-153X-7-41>
- [10] Tan, L.-L., Ong, W.-J., Chai, S.-P., Goh, B.T. and Mohamed, A.R. (2015) Visible-Light-Active Oxygen rich TiO₂ Decorated 2D Graphene Oxide with Enhanced Photocatalytic Activity toward Carbon Dioxide Reduction. *Applied Catalysis B: Environmental*, **179**, 160-170. <https://doi.org/10.1016/j.apcatb.2015.05.024>
- [11] Xiang, Q. and Jaroniec, M. (2011) Nanoscale Enhanced Photocatalytic H₂-Production Activity of Graphene-Modified Titania Nanosheets. *Nanoscale*, No. 9, 3670-3678. <https://doi.org/10.1039/c1nr10610d>
- [12] Tan, L.-L., Ong, W.-J., Chai, S.-P. and Mohamed, A.R. (2013) Reduced Graphene Oxide-TiO₂ Nanocomposite as a Promising Visible-Light-Active Photocatalyst for the Conversion of Carbon Dioxide. *Nanoscale Research Letters*, **8**, 465. <https://doi.org/10.1186/1556-276X-8-465>
- [13] Shen, J., Shi, M., Yan, B., Ma, H., Li, N. and Ye, M. (2011) Ionic Liquid-Assisted One-Step Hydrothermal Synthesis of TiO₂-Reduced Graphene Oxide Composites.

- Nano Research*, **4**, 795-806. <https://doi.org/10.1007/s12274-011-0136-7>
- [14] Perera, S.D., Mariano, R.G., Vu, K., Nour, N., Seitz, O., Chabal, Y. and Balkus, K.J. (1987) Hydrothermal Synthesis of Graphene-TiO₂ Nanotube Composites with Enhanced Photocatalytic Activity. *ACS Catalysis*, **2**, 949-956. <https://doi.org/10.1021/cs200621c>
- [15] Wang, M., Wang, D. and Li, Z. (2016) Self-Assembly of CPO-27-Mg/TiO₂ Nanocomposite with Enhanced Performance for Photocatalytic CO₂ Reduction. *Applied Catalysis B: Environmental*, **183**, 47-52. <https://doi.org/10.1016/j.apcatb.2015.10.037>
- [16] Zhang, Q., Lin, C.F., Jing, Y.H. and Chang, C.T. (2014) Photocatalytic Reduction of Carbon Dioxide to Methanol and Formic Acid by Graphene-TiO₂. *Journal of the Air & Waste Management Association*, **64**, 578-585. <https://doi.org/10.1080/10962247.2013.875958>
- [17] Fan, W., Lai, Q., Zhang, Q. and Wang, Y. (2011) Nanocomposites of TiO₂ and Reduced Graphene Oxide as Efficient Photocatalysts for Hydrogen Evolution. *The Journal of Physical Chemistry C*, **115**, 10694-10701.
- [18] Ali, S.M. (2014) Production of Nanosized Synthetic Rutile from Ilmenite Concentrate by Sonochemical HCl and H₂SO₄ Leaching. *Iranian Journal of Chemistry & Chemical Engineering—International English Edition*, **33**, 29-36.
- [19] Mukifza, A., Yusof, S., Awang, H. and Farid, E.M. (2016) Synthesis and Characterization of Titanium Dioxide Using a Caustic Hydrothermal with Moderate Molarity and Ratio from Synthetic Rutile Waste. *European Journal of Science and Technology*, **4**, 127-130.
- [20] Liang, D., Cui, C., Hu, H., Wang, Y., Xu, S., Ying, B., Li, P. and Lu, B. (2014) One-Step Hydrothermal Synthesis of Anatase TiO₂/Reduced Graphene Oxide Nanocomposites with Enhanced Photocatalytic Activity. *Journal of Alloys and Compounds*, **582**, 236-240. <https://doi.org/10.1016/j.jallcom.2013.08.062>
- [21] Sakthivel, S. and Kisch, H. (2003) Daylight Photocatalysis by Carbon-Modified Titanium Dioxide. *Angewandte Chemie International Edition*, **42**, 4908-4911.
- [22] Liang, Y.T., Vijayan, B.K., Gray, K.A. and Hersam, M.C. (2011) Minimizing Graphene Defects Enhances Titania Nanocomposite-Based Photocatalytic Reduction of CO₂ for Improved Solar Fuel Production. *Nano Letters*, **11**, 2865-2870.